



STOCHASTIC UPSCALING FOR WAVES IN POLYCRYSTALLINE MATERIALS

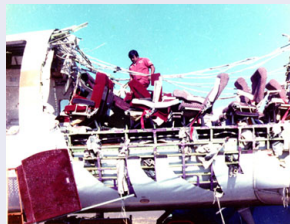
ROGER GHANEM ARASH NOSHADRAVAN

UNIVERSITY OF SOUTHERN CALIFORNIA

Description of the Problem

Prognosis

Anticipate damage from measured data :
determine requisite information,
number, type and location of sensors.



Description of the Problem

Prognosis

Anticipate damage from measured data :
determine requisite information,
number, type and location of sensors.



Challenge

- Damage initiates at a very small scale.



Description of the Problem

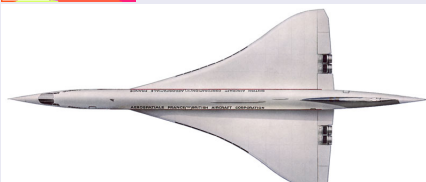
Prognosis

Anticipate damage from measured data :
determine requisite information,
number, type and location of sensors.



Challenge

- Damage initiates at a very small scale.
- Measured data is at a coarse scale.



Description of the Problem

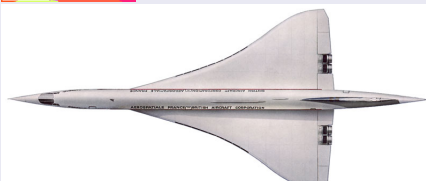
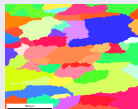
Prognosis

Anticipate damage from measured data :
determine requisite information,
number, type and location of sensors.



Challenge

- Damage initiates at a very small scale.
- Measured data is at a coarse scale.
- The details of the microscale for the specimen being measured are not known.



Microscale Simulation

- microstructure unknown - can be characterized statistically in the lab.
- to determine location of sensors we need to formulate an optimization problem.
- mechanistic analysis of an ensemble of microstructures is very expensive.

Solution

Develop a new stochastic mechanistic model with :

- State of the model at same scale as experimental observables (scale 1).
- Model behavior sensitive to occurrences at the scale of damage initiation (scale 2).
- Scatter in predictions from model consistent with observed scatter.
- Behavior of model honors known accepted conservation laws.

Part I

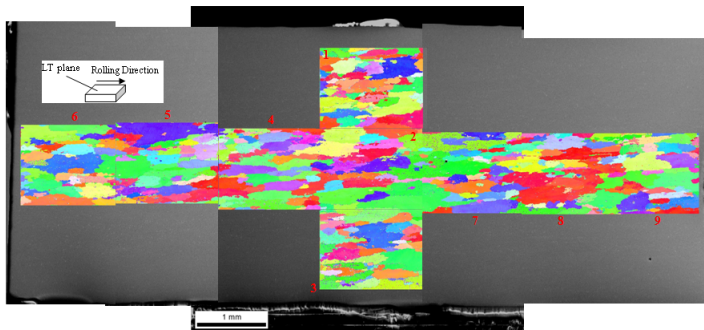
Simulation of random polycrystalline microstructure from experimental data

- Experimental database
- Simulation of random geometry
- Simulation of random material properties

I. Simulation of random polycrystals based on experimental data

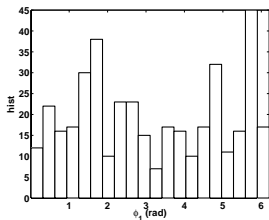
Experimental data

- EBSD map of 10X5 [mm] Al-2024
- 9 pictures (≈ 400 grains)
- Grain size, shape and crystallographic orientation $\Phi = [\phi_1, \phi, \phi_2]$

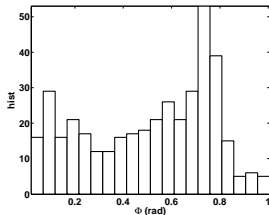


I. Simulation of random polycrystals based on experimental data

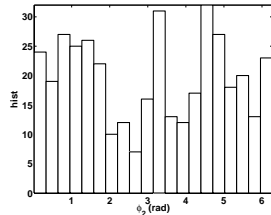
Statistics of grain geometry and crystallographic orientation obtained from EBSD



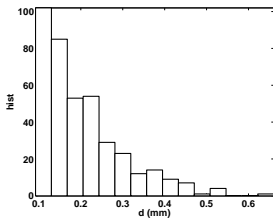
ϕ_1



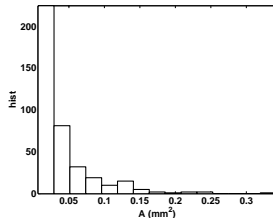
ϕ



ϕ_2



grain size



grain area

I. Simulation of random polycrystals based on experimental data

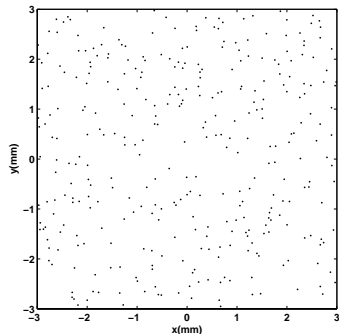
(A) Simulation of random geometry

I. Simulation of random polycrystals based on experimental data

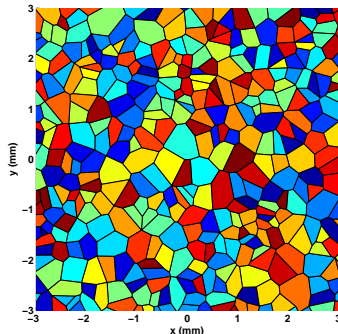
(A) Simulation of random geometry

2-D Voronoi-Polycrystal

- Poisson-Voronoi tessellation
- Parameterized by the intensity of underlying Poisson point process controlling the average grain size
- The usual tessellation is defined with respect to *Euclidean distance*



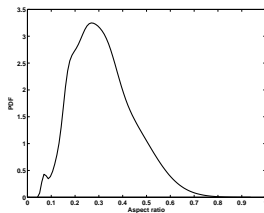
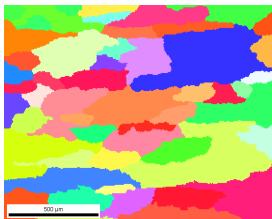
The underlying Poisson point process



A realization of Voronoi polycrystal

I. Simulation of random polycrystals based on experimental data

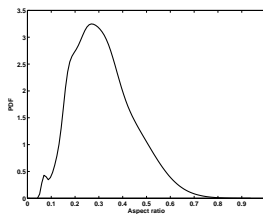
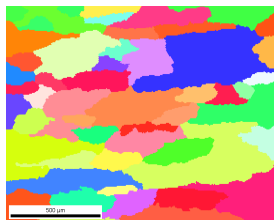
(A) Simulation of random geometry



- Classical Voronoi tessellation not capable of generating elongated grains !

I. Simulation of random polycrystals based on experimental data

(A) Simulation of random geometry



- Classical Voronoi tessellation not capable of generating elongated grains !

Voronoi-G tessellation (*T.H. Sheike, 1994*)

- Extension of classical Voronoi-tessellating by using the following distance

$$\mathcal{V}(\mathbf{x}_{tes}^{(i)}) \stackrel{\text{def}}{=} \{ \mathbf{x} \in \Omega \mid d_G(\mathbf{x}_{tes}^{(i)}, \mathbf{x}) \leq d_G(\mathbf{x}_{tes}^{(i)}, \mathbf{x}_{tes}^{(j)}) \}, \quad (1)$$

$$d_G(\mathbf{x}, \mathbf{y}) \stackrel{\text{def}}{=} \sqrt{(\mathbf{x}, \mathbf{y})^T [G] (\mathbf{x}, \mathbf{y})}$$

$$[G] = \begin{bmatrix} (1/g_x)^2 & 0 \\ 0 & (1/g_y)^2 \end{bmatrix}$$

- g_x (resp. g_y) : Rate of growth of tessellation in x (resp. y) direction.

I. Simulation of random polycrystals based on experimental data

(A) Simulation of random geometry

- Let $[G]$ be defined as,

$$[G] = \begin{bmatrix} (1/s)^2 & 0 \\ 0 & 1 \end{bmatrix}$$

Algorithm for generating Voronoi-G tessellation

- 1 Let $[Q] \leftarrow [G] = [Q]^T [Q]$
- 2 Generate homogenous Poisson point process $\mathbf{x}_{tes}^{(i)}$ with the desired intensity
- 3 Modify the coordinate of the points applying the transformation $\tilde{\mathbf{x}}_{tes}^{(i)} \leftarrow [Q] \mathbf{x}_{tes}^{(i)}$
- 4 Generate the classical Poisson Voronoi tessellation $\mathcal{V}(\tilde{\mathbf{x}}_{tes}^{(i)})$
- 5 Modify the coordinate of all the points $\mathbf{y} \in \mathcal{V}(\tilde{\mathbf{x}}_{tes}^{(i)})$ applying the transformation $\tilde{\mathbf{y}} \leftarrow [Q]^{-1} \mathbf{y}$

I. Simulation of random polycrystals based on experimental data

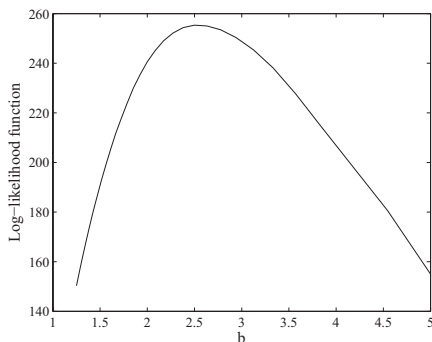
(A) Simulation of random geometry

Maximum likelihood estimation of the parameter s

$$\hat{s} = \arg \max_{b \in \mathbb{R}^+} \mathcal{L}(\omega_{exp}^{(1)}, \dots, \omega_{exp}^{(394)}, b),$$

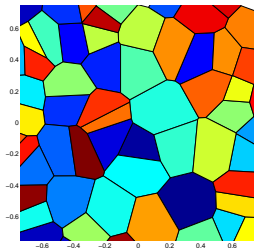
where \mathcal{L} represents the Log-Likelihood function defined as :

$$\mathcal{L}(\omega_{exp}^{(1)}, \dots, \omega_{exp}^{(394)}, b) = \sum_{i=1}^{394} \log(p_{\omega}(\omega_{exp}^i, b))$$

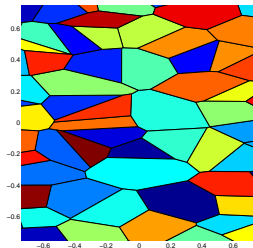


I. Simulation of random polycrystals based on experimental data

(A) Simulation of random geometry



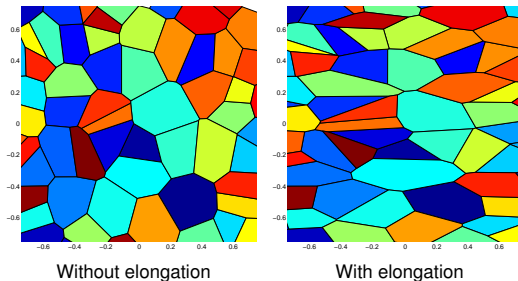
Without elongation



With elongation

I. Simulation of random polycrystals based on experimental data

(A) Simulation of random geometry



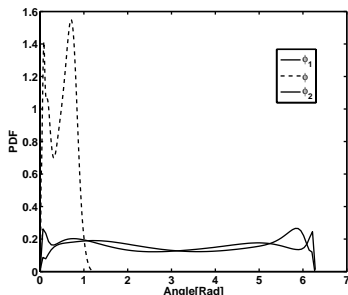
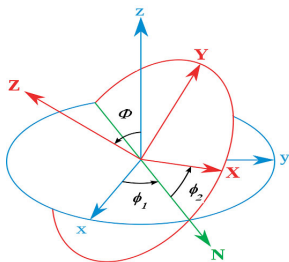
(B) Simulation of random properties

- Material properties are defined by
 - The set of Euler angles characterizing the crystallographic orientation of the grains
 - The elastic parameters of the single crystal

$$C^{(cub)} = \begin{pmatrix} C_{11} & C_{12} & C_{12} & 0 & 0 & 0 \\ C_{12} & C_{11} & C_{12} & 0 & 0 & 0 \\ C_{12} & C_{12} & C_{11} & 0 & 0 & 0 \\ 0 & 0 & 0 & C_{44} & 0 & 0 \\ 0 & 0 & 0 & 0 & C_{44} & 0 \\ 0 & 0 & 0 & 0 & 0 & C_{44} \end{pmatrix}.$$

I. Simulation of random polycrystals based on experimental data

(B) Simulation of random properties



- Sampling from the joint distribution of ϕ_1 , ϕ and ϕ_2 by prescribing :
 - Marginal cumulative distribution functions
 - Spearman's rank correlation matrix
- Computing the global elasticity tensor by applying the tensorial transformation :

$$\mathbb{C}_{i'j'k'l'} = R_{i'i} R_{j'j} R_{k'k} R_{l'l} \mathbb{C}_{ijkl}^{(cub)},$$

$$\mathbf{R} = \mathbf{R}(\phi_1, \phi, \phi_2)$$

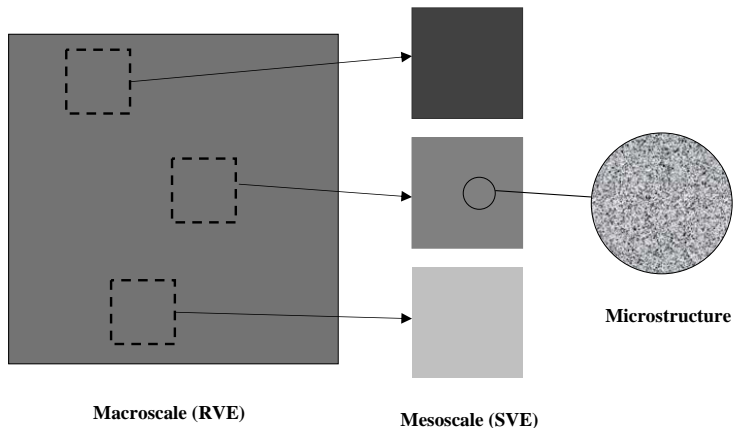
Part II

Nonparametric probabilistic modeling for upscaling uncertainty

- Overview of model construction
- Verification and validation
- Prognosis using wave propagation

II. Nonparametric probabilistic modeling for upscaling uncertainty

Definition of scales



II. Nonparametric probabilistic modeling for upscaling uncertainty

● Objective

- Mesoscale material description that (i) captures the effect of subscale heterogeneities and (ii) could be used in a coarse-scale modeling.
- Demonstrate the suitability of the resulting representation at detecting signatures of subscale damage.

II. Nonparametric probabilistic modeling for upscaling uncertainty

● Objective

- Mesoscale material description that (i) captures the effect of subscale heterogeneities and (ii) could be used in a coarse-scale modeling.
- Demonstrate the suitability of the resulting representation at detecting signatures of subscale damage.

● Approach : *Nonparametric probabilistic modeling*

- Constructing a probability distribution on the set of elasticity matrices.
- Constrain random matrices to specified physics-based bounds.
- Calibrate the random matrices from all the available information.

II. Nonparametric probabilistic modeling for upscaling uncertainty

Overview of model construction

Let :

$$\mathbf{N} = (\mathbf{C} - \mathbf{C}_l)^{-1} - (\mathbf{C}_u - \mathbf{C}_l)^{-1} > 0,$$

Maximize :

$$\int_{\mathbb{M}_n^+(\mathbb{R})} \ln(\rho) \rho_{\mathbf{N}}(N) dN$$

subject to :

$$\int_{\mathbb{M}_n^+(\mathbb{R})} \rho_{\mathbf{N}}(N) dN = 1,$$

$$\int_{\mathbb{M}_n^+(\mathbb{R})} N \rho_{[\mathbf{N}]}(N) dN = \underline{N} \in \mathbb{M}_n^+(\mathbb{R}),$$

$$\int_{\mathcal{C}} \ln(\det(N)) \rho_{\mathbf{N}}(N) dN = c_N, |c_N| < +\infty.$$

$$\rho_{\mathbf{N}}(N) = \mathbb{I}_{\mathbb{M}_n^+(\mathbb{R})}(\mathbf{N}) \hat{c}_0 \det(N)^{\lambda-1} \text{etr}\{-\Lambda_{\mathbf{N}} N\}$$

$\Lambda_{\mathbf{N}}$ and λ are Lagrange multipliers.

II. Nonparametric probabilistic modeling for upscaling uncertainty

Calibration

- Computing the realizations of the bounds for apparent elasticity matrix (Huet's partitioning technique)
- Computing the realizations of the apparent elasticity matrix

Apparent properties

$$\left. \begin{array}{l} \min \|\langle \sigma \rangle_{BC} - [C] \langle \epsilon \rangle_{BC} \| \\ \text{subject to meaningful constraints} \end{array} \right\} \Rightarrow [C^{app}]$$

BCs :

- *SUBC* : $\mathbf{t}(\mathbf{x}) = \sigma_0 \mathbf{n}(\mathbf{x}) \Rightarrow$ Lower bound $[C_{\sigma}^{app}]$
- *KUBC* : $\mathbf{u}(\mathbf{x}) = \epsilon_0 \mathbf{x} \Rightarrow$ Upper bound $[C_{\epsilon}^{app}]$
- *MBC* (*Tension test, e.g.*) \Rightarrow Samples of apparent elasticity tensor $[C^{app}]$

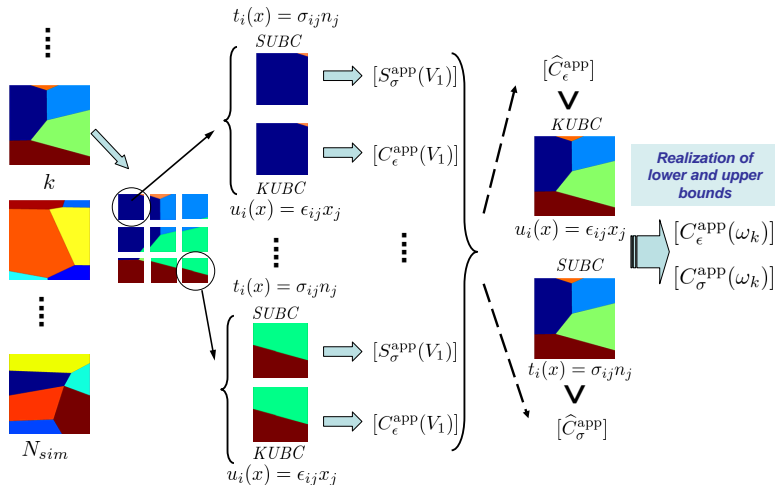
II. Nonparametric probabilistic modeling for upscaling uncertainty

Calibration

Huet's partitioning technique to obtain the realizations of the bounds :

- For the volume element smaller than RVE :

$$[\widehat{\mathbf{C}}_{\sigma}^{\text{app}}] \leq [\mathbf{C}_{\sigma}^{\text{app}}] \leq [\mathbf{C}_{\epsilon}^{\text{app}}] \leq [\widehat{\mathbf{C}}_{\epsilon}^{\text{app}}],$$



II. Nonparametric probabilistic modeling for upscaling uncertainty

Calibration

Step 1 : Compute the deterministic bounds

$$[C_l] = \arg \min_{[C] \in \mathcal{C}_l} \sum_{k=1}^{N_{sim}} \|C_{\sigma}^{\text{app}}(\omega_k) - [C]\|_F, \quad [C_u] = \arg \min_{[C] \in \mathcal{C}_u} \sum_{k=1}^{N_{sim}} \|[C] - C_{\epsilon}^{\text{app}}(\omega_k)\|_F$$

II. Nonparametric probabilistic modeling for upscaling uncertainty

Calibration

Step 1 : Compute the deterministic bounds

$$[C_l] = \arg \min_{[C] \in \mathcal{C}_l} \sum_{k=1}^{N_{sim}} \|C_{\sigma}^{app}(\omega_k) - [C]\|_F, \quad [C_u] = \arg \min_{[C] \in \mathcal{C}_u} \sum_{k=1}^{N_{sim}} \|[C] - C_{\epsilon}^{app}(\omega_k)\|_F$$

Step 2 : Compute the realization of apparent elasticity matrix (Tension test)

$$[C^{app}] = \arg \min_{[C_l] < [C] < [C_u]} \|\langle \sigma \rangle_{MBC} - [C] \langle \epsilon \rangle_{MBC}\|$$

II. Nonparametric probabilistic modeling for upscaling uncertainty

Calibration

Step 1 : Compute the deterministic bounds

$$[C_l] = \arg \min_{[C] \in C_l} \sum_{k=1}^{N_{sim}} \|C_{\sigma}^{app}(\omega_k) - [C]\|_F, \quad [C_u] = \arg \min_{[C] \in C_u} \sum_{k=1}^{N_{sim}} \|[C] - C_{\epsilon}^{app}(\omega_k)\|_F$$

Step 2 : Compute the realization of apparent elasticity matrix (Tension test)

$$[C^{app}] = \arg \min_{[C_l] < [C] < [C_u]} \|\langle \sigma \rangle_{MBC} - [C] \langle \epsilon \rangle_{MBC}\|$$

Step 3 : Compute the statistical estimates of parameters for $N_{sim} = 100$ and $\Omega = 0.3 \times 0.3$ [mm]

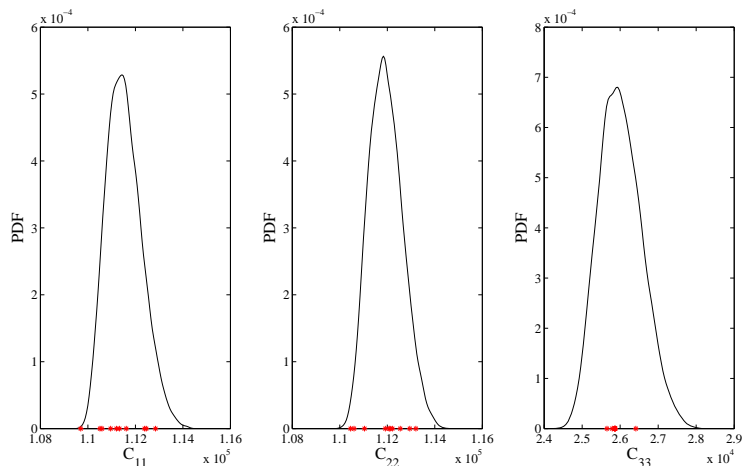
$$\tilde{\delta}_N = \left\{ \frac{1}{N_{sim} \|[\tilde{N}]\|_F^2} \sum_{k=1}^{N_{sim}} \|[N(\omega_k)] - [\tilde{N}]\|_F^2 \right\}^{1/2} = 0.66$$

$$[\tilde{N}] = \frac{1}{N_{sim}} \sum_{k=1}^{N_{sim}} [N(\omega_k)] = 10^{-3} \begin{bmatrix} 0.2667 & 0.0879 & -0.0189 \\ 0.0879 & 0.2214 & 0.0277 \\ -0.0189 & 0.0277 & 0.2366 \end{bmatrix}$$

II. Nonparametric probabilistic modeling for upscaling uncertainty

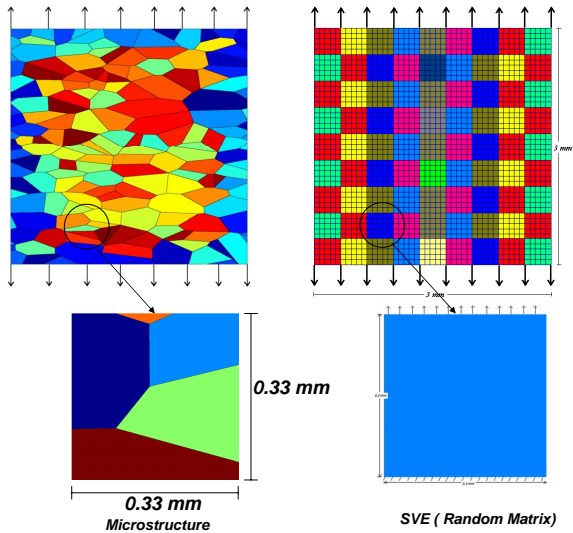
Verification

Whether or not the model implementation accurately represent the intended conceptual description of the model and the solution to the model



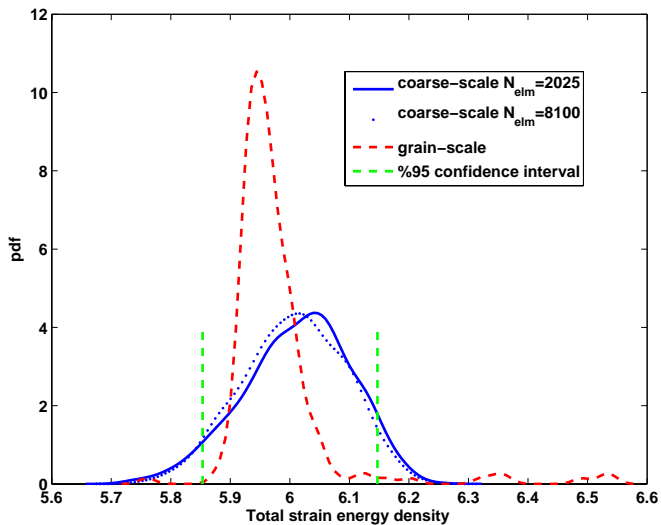
II. Nonparametric probabilistic modeling for upscaling uncertainty

Validation



II. Nonparametric probabilistic modeling for upscaling uncertainty

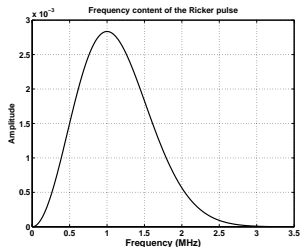
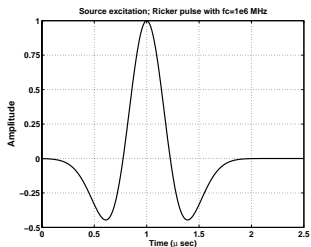
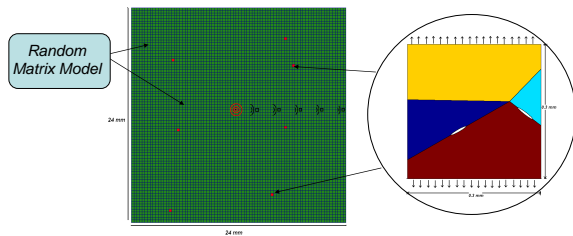
Validation



II. Nonparametric probabilistic modeling for upscaling uncertainty

Damage detection

The FE model and applied excitation :



II. Nonparametric probabilistic modeling for upscaling uncertainty

Characterization of the scattered waves due to heterogeneity

- Elastodynamic response of linear elastic material :

$$\left\{ \delta_{jk} \rho(\mathbf{x}) \frac{\partial^2}{\partial t^2} + \frac{\partial}{\partial x_i} C_{ijkl}(\mathbf{x}) \frac{\partial}{\partial x_l} \right\} G_{k\alpha}(\mathbf{x}, \mathbf{x}'; t) = \delta_{j\alpha} \delta^3(\mathbf{x} - \mathbf{x}') \delta(t).$$

- Let $\mathbf{u}^i(t) = \langle \mathbf{u}(t) \rangle^i + \mathbf{u}'^i(t)$.
- Each particular realization of the scattered waveform has different pattern of fluctuations around the mean response.
- The random fluctuations contain information on sub-scale heterogeneities.

II. Nonparametric probabilistic modeling for upscaling uncertainty

Characterization of the scattered waves due to heterogeneity

- Elastodynamic response of linear elastic material :

$$\{\delta_{jk}\rho(\mathbf{x})\frac{\partial^2}{\partial t^2} + \frac{\partial}{\partial x_i}C_{ijkl}(\mathbf{x})\frac{\partial}{\partial x_l}\}G_{k\alpha}(\mathbf{x}, \mathbf{x}'; t) = \delta_{j\alpha}\delta^3(\mathbf{x} - \mathbf{x}')\delta(t).$$

- Let $\mathbf{u}^i(t) = \langle \mathbf{u}(t) \rangle^i + \mathbf{u}'^i(t)$.
- Each particular realization of the scattered waveform has different pattern of fluctuations around the mean response.
- The random fluctuations contain information on sub-scale heterogeneities.

- The energy of the wave is characterized by the intensity defined as :

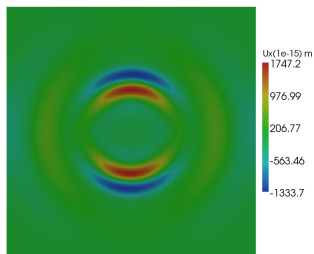
$$I_{u_k^i(t)} = \int_T (u_k^i(t))^2 dt.$$

- A scalar-valued random variable η^i is defined to characterize the fluctuation :

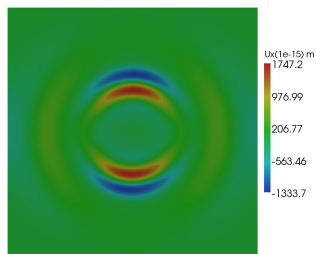
$$\eta^i = \frac{I_{\mathbf{u}'^i(t)}}{I_{\langle \mathbf{u}_k^i(t) \rangle}}.$$

II. Nonparametric probabilistic modeling for upscaling uncertainty

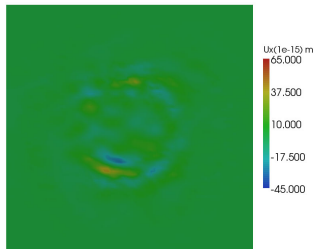
Snapshots of the mean displacement field and a typical fluctuation



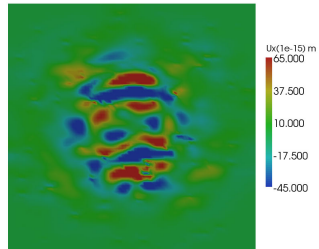
mean field $\langle \mathbf{u}(t) \rangle$ - healthy



mean field $\langle \mathbf{u}(t) \rangle$ - damaged



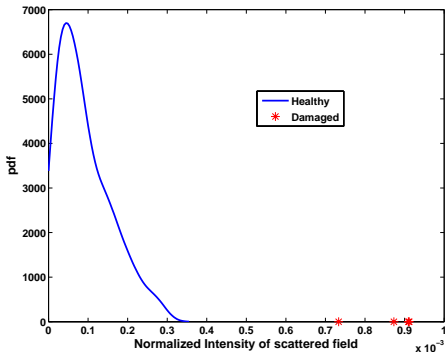
a realization of $\mathbf{u}'(t)$ - healthy



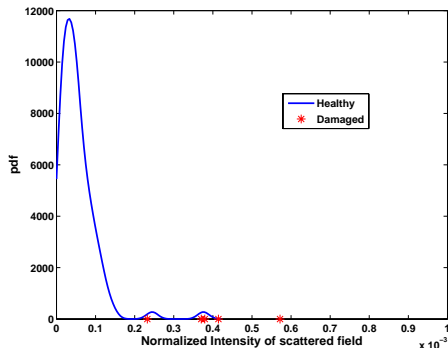
a realization of $\mathbf{u}'(t)$ - damaged

II. Nonparametric probabilistic modeling for upscaling uncertainty

Probability density function of η at different receivers



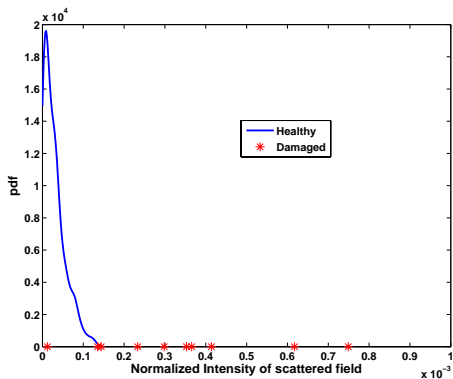
Receiver 1 @ $x = 2.4\text{mm}$



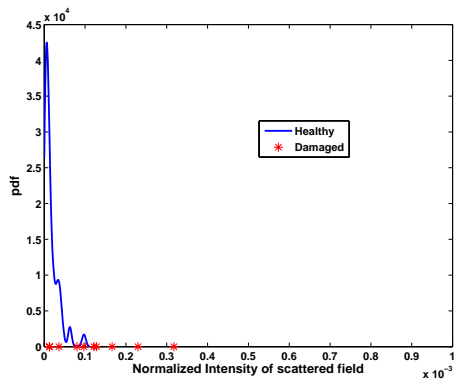
Receiver 2 @ $x = 4.8\text{mm}$

II. Nonparametric probabilistic modeling for upscaling uncertainty

Probability density function of η at different receivers



Receiver 3 @ $x = 7.2mm$



Receiver 4 @ $x = 9.6mm$

Validation of Random Matrix Model

Attenuation coefficient α :

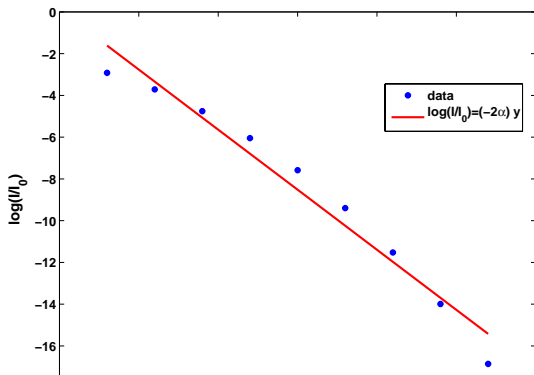
- The energy of the wave is characterized by the intensity defined as :

$$I(y) = \int_T (\mathbf{u}(y, t))^2 dt.$$

- Attenuation coefficient α is defined as the rate of exponential decay in the intensity of the waves :

$$I(y) = I_0 e^{-2\alpha y},$$

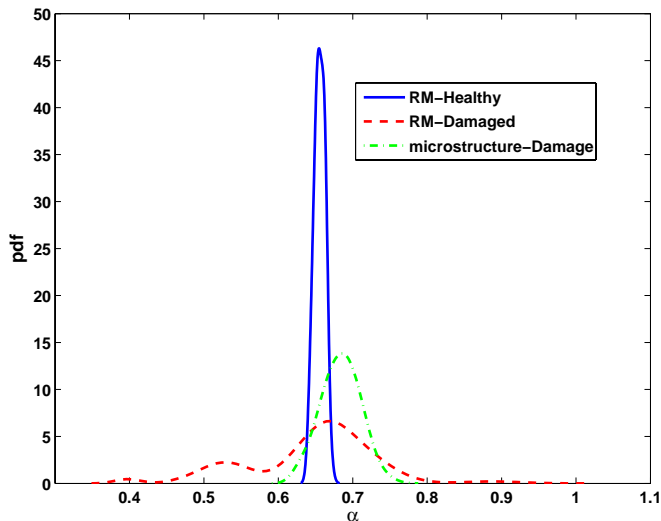
where I_0 is the intensity of the excitation.



Validation of Random Matrix Model

pdf of attenuation coefficient

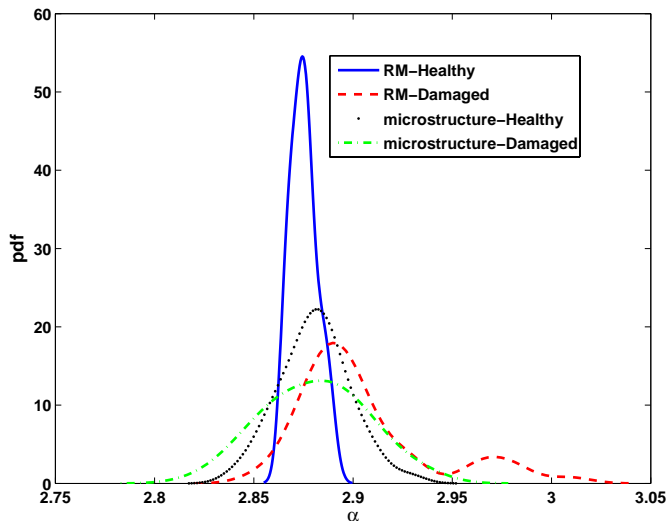
- Central frequency $f_c = 10\text{MHz}$



Validation of Random Matrix Model

pdf of attenuation coefficient

- Central frequency $f_c = 2\text{MHz}$



Part III

Wave propagation in random polycrystals

- Influence of inherent heterogeneity
- Influence of intergranular micro-cavities

III. Wave propagation in random polycrystals

Motivation

Review

- Ultrasonic measurements are used for material characterization, detection of anomaly, etc.
- Wave Scattering is usually characterized by attenuation and dispersion.
- Scattering models are often oversimplified.
- Not accurate enough in complex microstructure and for high-frequency regime.

III. Wave propagation in random polycrystals

Motivation

Review

- Ultrasonic measurements are used for material characterization, detection of anomaly, etc.
- Wave Scattering is usually characterized by attenuation and dispersion.
- Scattering models are often oversimplified.
- Not accurate enough in complex microstructure and for high-frequency regime.

Objective

- Present a fine scale numerical model for wave propagation in random polycrystals.
- Study the effect of random heterogeneity in ultrasonic waves.

III. Wave propagation in random polycrystals

Motivation

Review

- Ultrasonic measurements are used for material characterization, detection of anomaly, etc.
- Wave Scattering is usually characterized by attenuation and dispersion.
- Scattering models are often oversimplified.
- Not accurate enough in complex microstructure and for high-frequency regime.

Objective

- Present a fine scale numerical model for wave propagation in random polycrystals.
- Study the effect of random heterogeneity in ultrasonic waves.

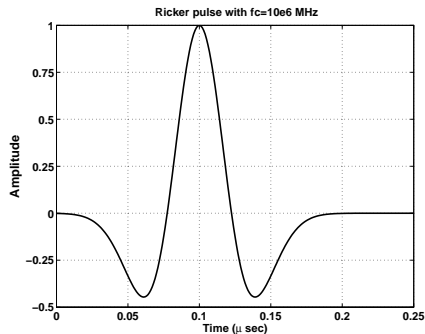
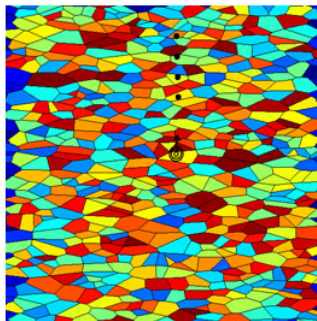
Application

- Validate theoretical scattering model in well-controlled microstructure.
- Circumvent limitation of experimental measurement.
- Facilitate interpretation of ultrasonic measurements.

III. Wave propagation in random polycrystals

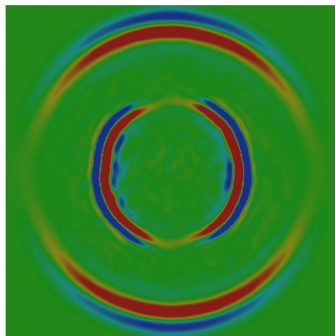
Numerical model

- 6×6 [mm] 2-D models of random Voronoi-G polycrystals are generated
- Each model consists of, roughly, 800 grains
- The models are discretized into the finite plane-strain triangular elements
- The time integration scheme based on Newark- β method is implemented in *Trilinos* for simulation of wave propagation
- The waveforms are obtained in an array of receivers due to the applied Ricker pulse in the the center

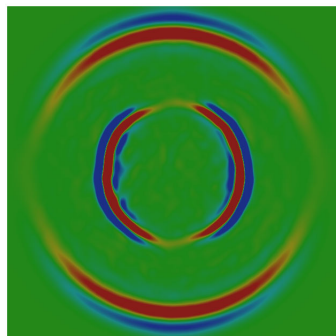


III. Wave propagation in random polycrystals

Stability of solution with respect to the FE discretization



maximum element size= $0.1\lambda_c$



maximum element size= $0.05\lambda_c$

- λ_c : wavelength corresponding to the central frequency of excitation

Element size	Number of nodes	Num. of processors	Processor type	Comp. time
$0.1\lambda_c$	71737	36	2GB 3.2GHz	3 min.
$0.05\lambda_c$	271900	36	2GB 3.2GHz	16 min.

III. Wave propagation in random polycrystals

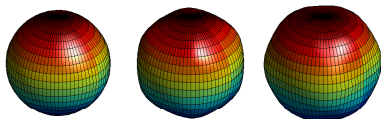
Influence of inherent heterogeneity

- The single crystal for both Al and Copper present a cubic material symmetry
- The anisotropy elasticity matrix has 9 plane of symmetry and depends on 3 parameters

$$C^{(cub)} = \begin{pmatrix} C_{11} & C_{12} & C_{12} & 0 & 0 & 0 \\ C_{12} & C_{11} & C_{12} & 0 & 0 & 0 \\ C_{12} & C_{12} & C_{11} & 0 & 0 & 0 \\ 0 & 0 & 0 & C_{44} & 0 & 0 \\ 0 & 0 & 0 & 0 & C_{44} & 0 \\ 0 & 0 & 0 & 0 & 0 & C_{44} \end{pmatrix}$$

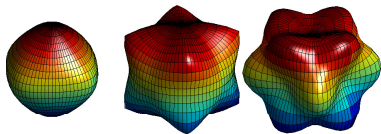
- The level of anisotropy is characterized by Zener index : $A = 2C_{44}/(C_{11} - C_{12})$.
- $A_{Al} = 1.2 \Rightarrow$ roughly isotropic

Slowness surface for Al :



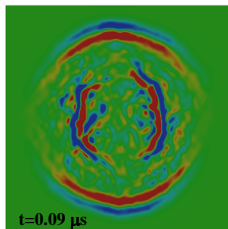
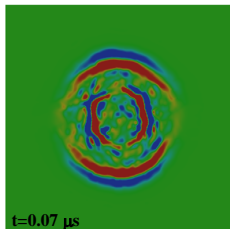
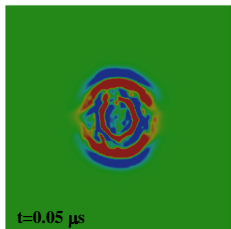
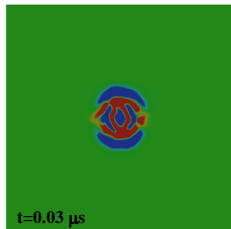
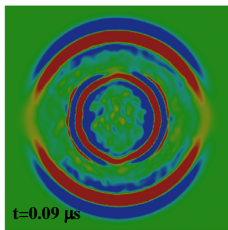
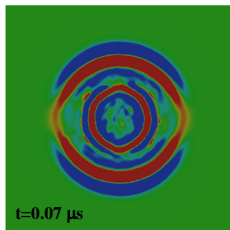
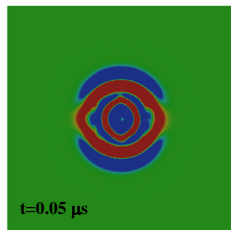
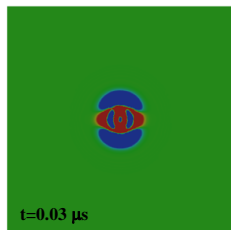
- $A_{cop} = 3.2 \Rightarrow$ highly anisotropic

Slowness surface for copper :



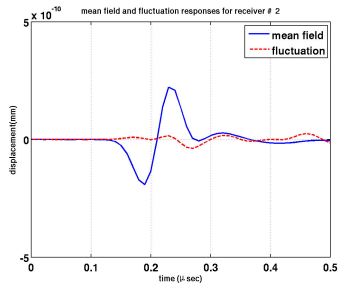
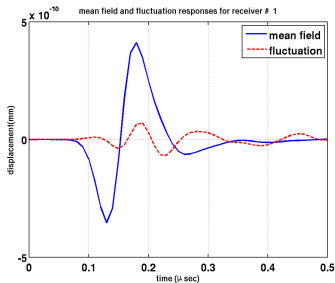
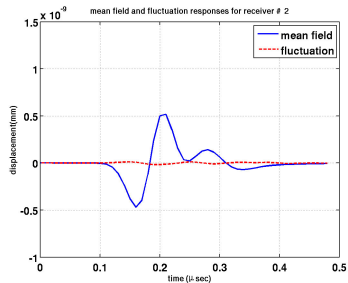
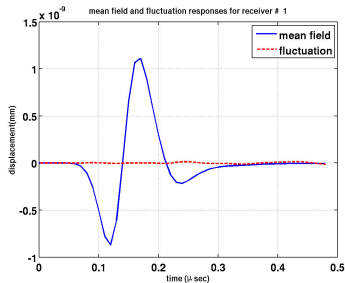
III. Wave propagation in random polycrystals

Snapshots of displacement fields in Al and Copper



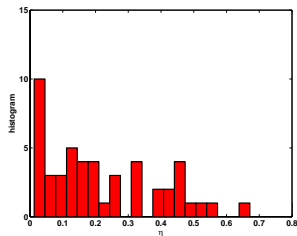
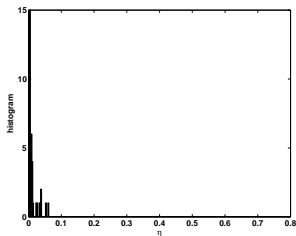
III. Wave propagation in random polycrystals

Mean waveform and the fluctuation in one realization for Al and Copper

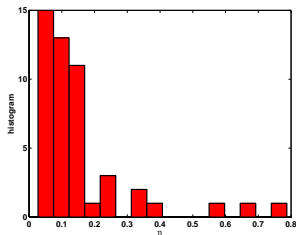
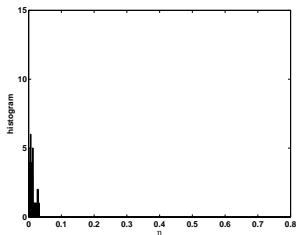


III. Wave propagation in random polycrystals

- Histograms of η at $y=0.3$ mm for Al. and Copper :

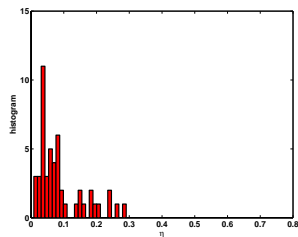
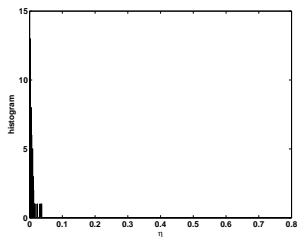


- Histograms of η at $y=0.9$ mm for Al. and Copper :

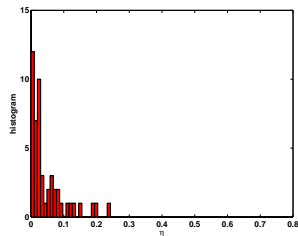
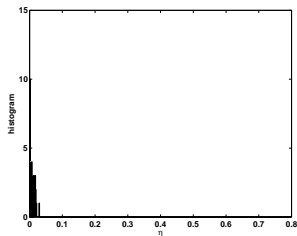


III. Wave propagation in random polycrystals

- Histograms of η at $y=1.5$ mm for Al. and Copper :



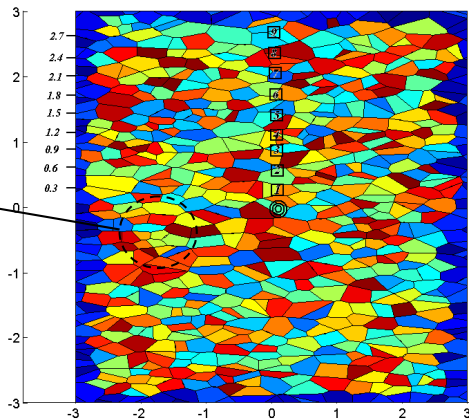
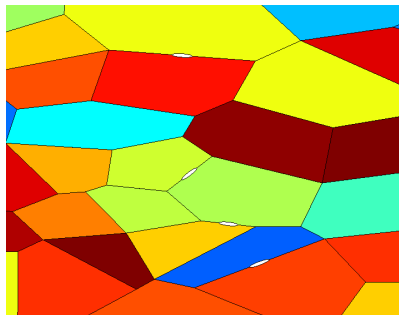
- Histograms of η at $y=2.1$ mm for Al. and Copper :



III. Wave propagation in random polycrystals

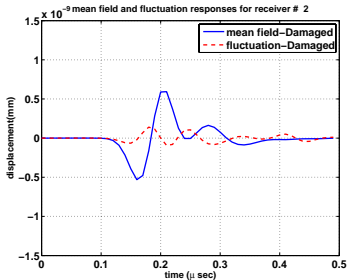
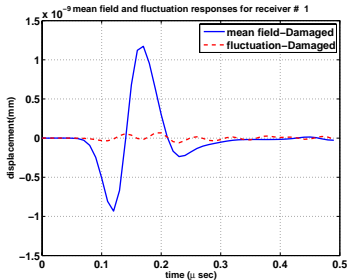
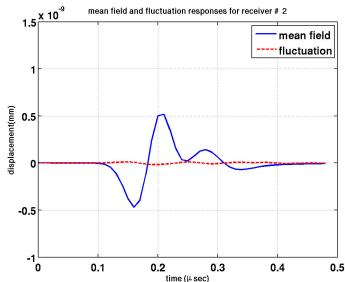
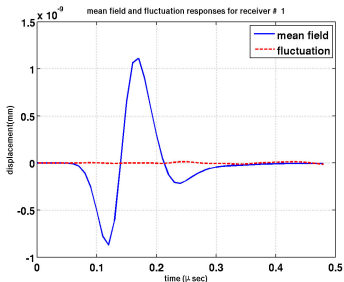
Influence of Intergranular micro-cavities

- Damage is introduced as ellipsoidal micro-cavities randomly inserted along the grain boundaries
- Void ratio of micro-cavities $\simeq 0.1\%$
- Aspect ratio of random ellipsoidal cavities : 0.2



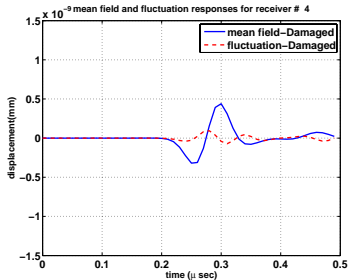
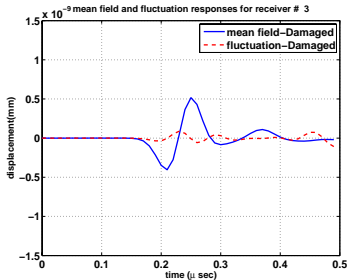
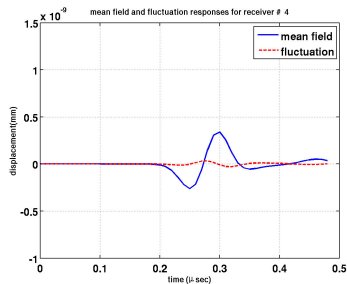
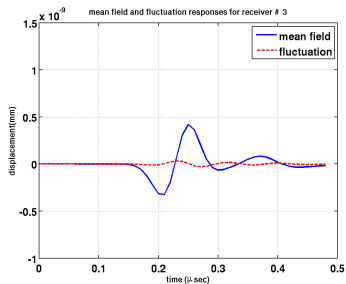
III. Wave propagation in random polycrystals

Mean waveform and a realization of fluctuation for **Aluminum**



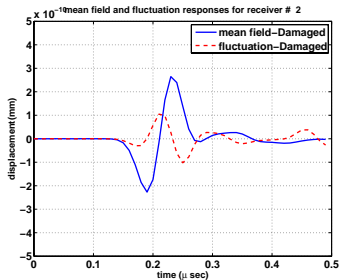
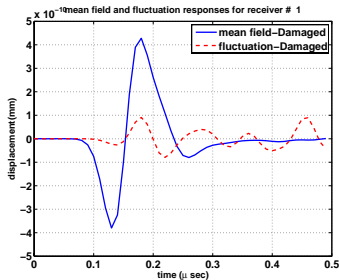
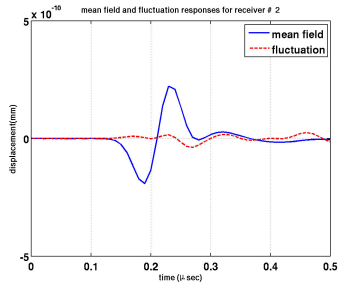
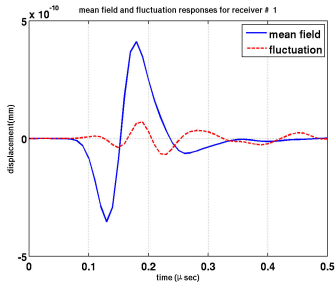
III. Wave propagation in random polycrystals

Mean waveform and a realization of fluctuation for **Aluminum**



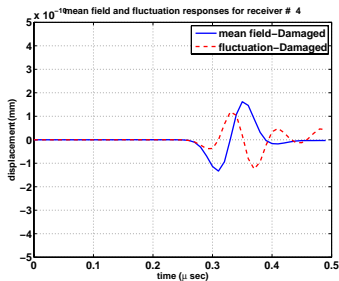
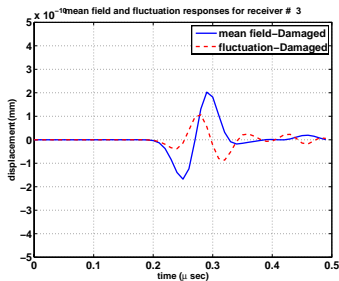
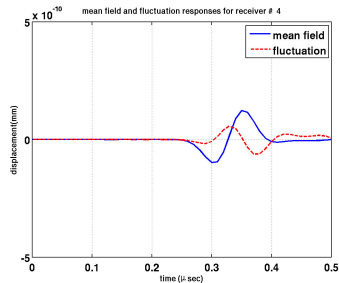
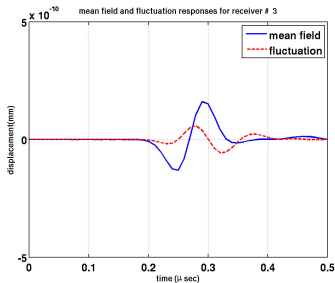
III. Wave propagation in random polycrystals

Mean waveform and a realization of fluctuation for Copper



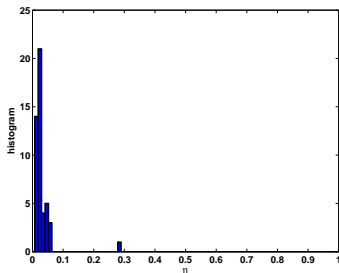
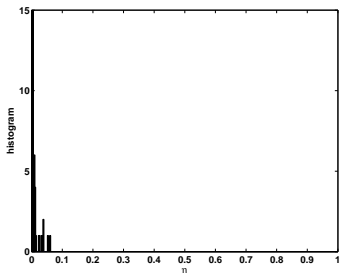
III. Wave propagation in random polycrystals

Mean waveform and a realization of fluctuation for Copper

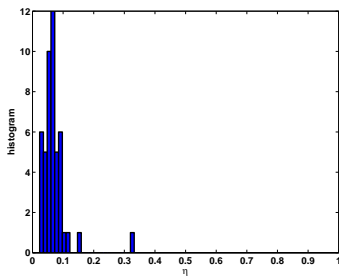
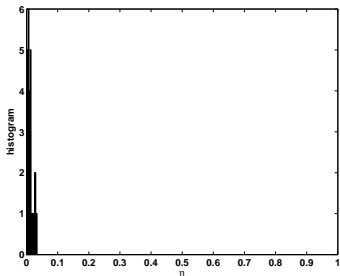


III. Wave propagation in random polycrystals

- Histograms of η at $y=0.3$ mm for *healthy* and *damaged* Aluminum :

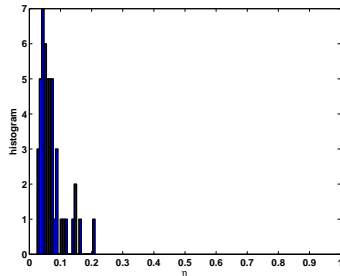
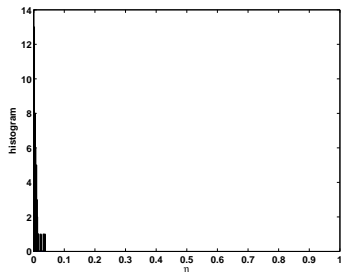


- Histograms of η at $y=0.9$ mm for *healthy* and *damaged* Aluminum :

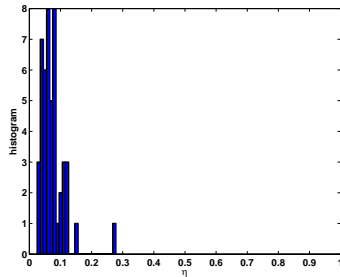
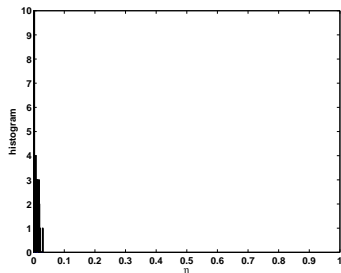


III. Wave propagation in random polycrystals

- Histograms of η at $y=1.5$ mm for *healthy* and *damaged* Aluminum :

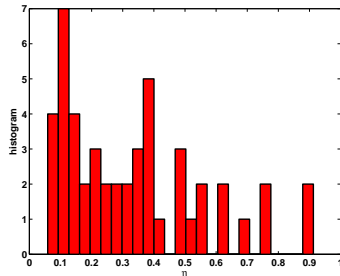
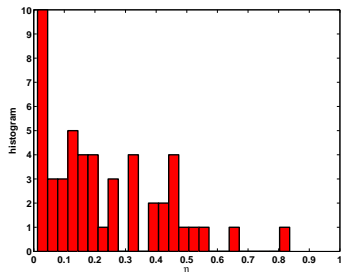


- Histograms of η at $y=2.1$ mm for *healthy* and *damaged* Aluminum :

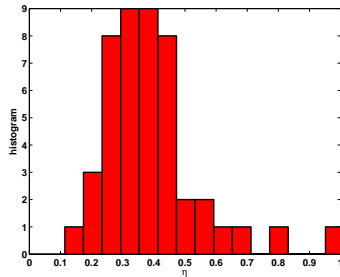
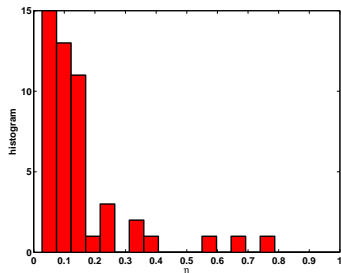


III. Wave propagation in random polycrystals

- Histograms of η at $y=0.3$ mm for *healthy* and *damaged* Copper :

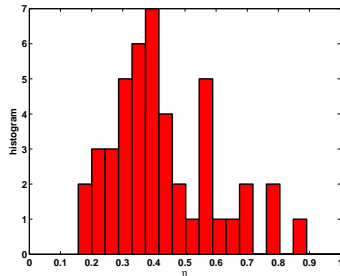
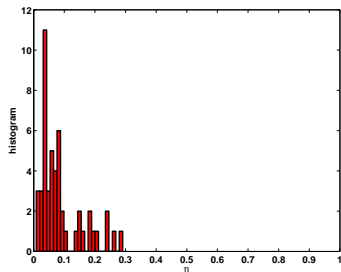


- Histograms of η at $y=0.9$ mm for *healthy* and *damaged* Copper :



III. Wave propagation in random polycrystals

- Histograms of η at $y=1.5$ mm for *healthy* and *damaged* Copper :



- Histograms of η at $y=2.1$ mm for *healthy* and *damaged* Copper :

